ACI STRUCTURAL JOURNAL TECHNICAL PAPER

Title no. 99-S68

Seismic Design of Columns with High-Strength Wire and Strand as Spiral Reinforcement

by A. M. Budek, M. J. N. Priestley, and Chin Ok Lee

Nine model concrete bridge columns using prestressing strand as transverse reinforcement were tested to establish design parameters for the use of high-strength transverse reinforcement under seismic loading. Five of these columns were tested to examine shear behavior, and four were tested to examine flexural behavior. One shear test and two flexural tests were dynamic. Moderate volumetric ratios (less than half of the ATC-32-specified value for Grade 60) of high-strength steel provided satisfactory performance under shear-critical conditions. The confinement of flexural hinges was satisfactory at reinforcement levels below that called for by the California Department of Transportation Bridge Design Specifications, provided that the spiral pitch was small enough to prevent buckling of the longitudinal reinforcement. Dynamic loading did not have any unanticipated effect on either shear or flexural performance.

Keywords: confinement; experimental; flexure; prestressing; reinforcement; shear.

INTRODUCTION

Reinforced concrete bridge columns subject to high shear demand may require a high volumetric ratio of transverse reinforcement to provide adequate shear strength. Seismic design generally implies a requirement for ductile response through which adequate shear strength must be maintained. Shear strength is carried by aggregate interlock in the concrete, by dowel action of the longitudinal reinforcement, and by truss action in the transverse reinforcement. It is enhanced by axial compression. As the structure passes into the inelastic range, the opening of wide shear cracks in the concrete degrades the competence of the aggregate interlock. The reinforcing steel will therefore be mobilized to a greater degree than would be implied by elastic analysis, and the contribution of the transverse reinforcement to the shear strength in a ductile response is a direct function of the volumetric transverse reinforcement ratio. However, high transverse reinforcement ratios and the ensuing steel congestion are undesirable both from constructibility and economic aspects, and may result in premature spalling of cover concrete.

The ATC-32 seismic bridge design standards[1] specify a force-reduction factor Z lower than that specified by the Caltrans BDS,[2] thereby imposing higher design force levels. In light of this, the adoption in ATC-32 of a shear model considerably more conservative than that used in the BDS[3] can result in structures that are, in their detailing requirements, difficult to build.

Consider a bridge column with a diameter of 2.44 m and a longitudinal reinforcement ratio $\rho_l = 0.02$. Material strengths for seismic design were taken as $f'_{ce} = 35.9$ MPa, $f_{ye} = 455$ MPa, and $f_{yt} = 413$ MPa (based on $f'_c = 27.6$ MPa and $f_{yt,yl} = 413$ MPa). For an axial load of $0.10 f'_c A_g$, the nominal moment capacity would be 55,285 kN-m. For a column height of $h_c = 9.75$ m, the aspect ratio would be 4 in the transverse direction of bending (normal to the bridge longitudinal axis, and thus in single bending) and 2 in the longitudinal direction (in which direction the rotational stiffness of the bridge superstructure puts the column into double bending).

The design shear force is[1]

$$V^0 = 2 \times 1.4 \frac{M_n}{h_c} = 15{,}877 \text{ kN} \quad (1)$$

The required shear capacity is

$$\frac{V^0}{\Phi} = \frac{15{,}877}{0.85} = 18{,}678 \text{ kN} \quad (2)$$

Under ATC-32, the concrete contribution to the shear strength in a plastic hinge is

$$V^0 = 0.166\left[0.5 + \frac{P_e}{13.8A_g}\right]\sqrt{f'_c}\,(0.8A_g)(\text{MPa units}) \quad (3)$$

and the reinforcement contribution by

$$V_s = \frac{\pi}{2}\frac{A_h f_{yt} D'}{s} \quad (4)$$

The concrete contribution is thus 2276 kN, and the required reinforcement contribution is 16,402 kN. With $f_{yt} = 413$ MPa, this requires a volumetric ratio of transverse reinforcement of. This is impractical: the close spiral spacing (14.5 mm using No. 6 bar) will hinder placement of concrete. If larger bar sizes were used, they would have to be placed as welded hoops, or lapped every 2.4 turns if the spiral was made from standard 18.3 m (60 ft) long bars (for No. 7 bar and higher). Neither solution is attractive, as welds are subject to failure, and lapping leads to more congestion.

The fact that the previously described approach results in an impracticable solution is due in part to the limitation on allowable stress in transverse reinforcement to 413 MPa.[4] This arises from the requirement to control crack widths under service loads; however, the need to limit service load cracking is probably inappropriate for transitory effects such as seismic loading. Column shear retrofit design using composite materials

ACI Structural Journal, V. 99, No. 5, September-October 2002.
MS No. 01-313 received September 30, 2001, and reviewed under Institute publication policies. Pertinent discussion will be published in the July-August 2003 *ACI Structural Journal* if received by March 1, 2003.

A. M. Budek *is an assistant professor of technology at Southwest Texas State University. His interests include seismic design of reinforced concrete bridge and building components, experimental and analytical modeling of soil-structure interaction, and composite retrofit design methodology.*

M. J. N. Priestley, *FACI, is a Professor Emeritus at the University of California at San Diego. He received ACI's Raymond C. Reese Award in 1984 and 1989, and ACI's Wason and Anderson Awards in 1997. His research interests include seismic design, assessment, and retrofit of reinforced concrete bridges and buildings, seismic design philosophy for precast concrete structures, and development of realistic dynamic testing methods to simulate inelastic response under seismic loading.*

Chin Ok Lee *is an associate professor in the civil engineering department in Chungnam University, Daejon, Korea. His interests include seismic analysis, design, and retrofit of bridge structures, safety and seismic assessment of existing structures, and experimental seismic performance study of structures.*

at design transverse strains as high as 0.6%—approximately three times the strain limit implied by current code restrictions (and hence implying much higher curvatures)—have performed satisfactorily.[5] If the stress limitation of 413 MPa on transverse reinforcement were to be lifted, implying the use of high-strength reinforcement, the congestion described previously could be greatly alleviated.

A growing interest in the use of high-strength concrete (HSC) has led to investigations of high-strength confinement to fully exploit HSC's full capacity.[6-11] These investigations have used either high-strength wire or a deformed high-strength bar.

The use of multi-wire prestressing strand offers several advantages. Prestressing strand is available in a number of diameters, is manufactured in long lengths, and is flexible enough to be wrapped around a column cage. It is also less expensive, on a strength basis (per MPa), than a Grade 60 reinforcement.

With the large diameters and high volumetric ratios of transverse reinforcement required by recent design recommendations,[1,4] use of prestressing strand at a higher allowable stress should reduce congestion of steel.

RESEARCH SIGNIFICANCE

Current code seismic requirements for transverse reinforcement in spirally confined bridge columns such as those adopted in ATC-32 can result in severe congestion of reinforcing steel. This is exacerbated by the need to keep transverse reinforcement at or below a stress level of 413 MPa to control crack width. The present study shows that the use of high-strength reinforcing steel can significantly reduce the volumetric ratio of transverse reinforcement if a higher tensile stress is permitted, with performance equivalent or superior to that offered by conventional reinforcement.

PREVIOUS EXPERIMENTAL WORK

The use of HSC has driven research into the behavior of members confined with high-strength transverse reinforcement. High confining pressures are required to achieve an adequate increase in ductility for seismic design using HSC. These can be achieved either through increasing the volumetric transverse reinforcement ratio, or using higher-strength transverse reinforcement.

Previously tested column sections are compared with that used in the present test program in Fig. 1.

Axial compression tests

Pessiki, Graybeal, and Mudlock[6]—A procedure for the design and analysis of high-strength reinforcement was developed and validated through a number of large-scale axial compression tests. The design criterion used for detailing the spiral reinforcement was usable strength. Spiral reinforcement yield strength ranged from 538 to 1345 MPa, and the usable values ranged from 545 to 1131 MPa. The method showed good correlation between prediction and experiment for spirals with usable stress values below 758 MPa.

Li, Park, and Tanaka[7]—Li, Park, and Tanaka tested a large number of square and circular columns under axial load, with normal (f_{yt} = 445 MPa) and high-strength (f_{yt} = 1318 MPa) transverse reinforcement. The use of high-strength reinforcement generally enhanced the axial strength and ultimate compression strain of the confined concrete. The researchers noted that, while transverse bar yield stress may be used in calculating confining pressure for normal-strength reinforcement, it may not be accurate for high-strength reinforcement.

High-strain-rate axial loading (strain rate of 0.0167/s) showed that, while normal-strength confinement enhanced the core concrete strength, high-strength confinement did not.

Razvi and Saatcioglu[8]—Twenty-two circular cylinders of 250 mm diameter were tested under monotonic axial compression. High-strength concrete (60 to 120 MPa) was used. Yield strength of transverse reinforcement ranged from 400 to 1000 MPa. The proclivity of HSC to brittle failure could be ameliorated by providing sufficient confining pressure (proportional to $f_{yt}\rho_t$). The authors observed that increasing the spiral pitch of the transverse reinforcement increased the required confining pressure.

Flexural tests of rectangular columns

Muguruma et al.[9]—Four 200 mm square columns were tested. Two specimens were reinforced with 6 mm deformed bars (f_{yt} = 408 MPa); the other two were reinforced with 6 mm deformed bars with a yield stress of 873 MPa. The reinforcing hoops were butt-welded. Axial loads were 0.343 and $0.473f_c'A_g$.

The use of high-strength reinforcement did not increase flexural ductility at lower axial loads. However, improvement was seen at the higher axial load. Longitudinal bar buckling was delayed in the specimen using high-strength reinforcement.

Sato, Tanaka, and Park[10]—Two columns 400 mm square were tested using high-strength transverse reinforcement (f_{yt} = 1368 MPa), and normal-strength longitudinal reinforcement. The columns were reinforced for shear and confinement according to NZS 3101.[11] A strength of 1275 MPa was used for designing the transverse reinforcement.

The transverse reinforcement remained well within its elastic range into high ductility levels (normal-strength reinforcement would have yielded). Buckling of the longitudinal bars was also forestalled.

Li, Park, and Tanaka[7]—Cyclic lateral loading was carried out on three square-section columns using HSC. Moderate-to-high axial load levels were tested. Ductile behavior was not achieved in the plastic hinge regions. It was suggested that the lower dilation of high-strength concrete prevented the full mobilization of high-strength confinement. A maximum usable yield stress of 900 MPa was proposed for use in design equations.

Aziznamini and Saatcioglu[12]—Two 305 mm square columns were tested with HSC and high-strength (f_{yt} = 827 MPa) transverse reinforcement. The use of high-strength confinement was not found to play a significant role in the columns' flexural response. Dilation of the HSC was not sufficient to fully mobilize the transverse steel. Also, increasing the transverse bar spacing to follow ACI minimum requirements based on yield strength could reduce the antibuckling support for the longitudinal bars.

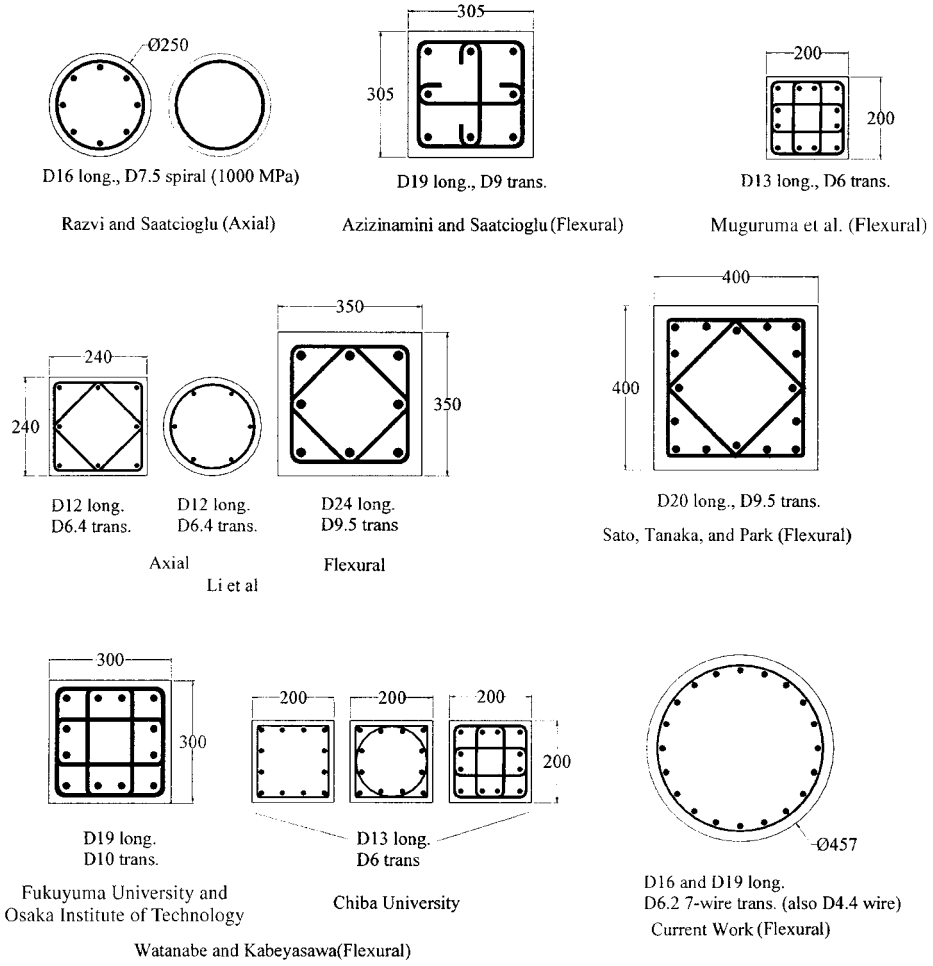

Fig. 1—Comparison of column section tested in present work, with previous research (dimensions in mm).

Watanabe and Kabeyasawa[13]—A number of low-aspect-ratio column tests were performed at the Osaka Institute of Technology, Fukuyama University, and Chiba University. The columns were square-section, and confined with either hoops or rectilinear ties, or spirals combined with rectilinear ties. The use of high-strength transverse reinforcement was generally found to enhance shear strength. Volumetric reinforcement ratio was significant.

The summary of work described previously shows that:

1. Under axial compression, high-strength transverse reinforcement enhances concrete compressive strength when compared with normal-strength reinforcement;
2. Axial loading rate did not have a significant effect on the performance of columns confined with high-strength transverse reinforcement;
3. Full utilization of the stress and strain capacity of high-strength transverse reinforcement may be limited by reduced dilation of HSC;
4. The higher yield strain of high-strength transverse reinforcement generally delayed the onset of longitudinal bar buckling; and
5. There is a lack of experimental data addressing the lateral load performance of spirally-confined circular columns using high-strength transverse reinforcement.

TESTING PROGRAM

This paper summarizes the results from a series of tests on spirally-confined columns, performed at the University of California, San Diego, using high-strength transverse reinforcement. The reinforcing material chosen was Grade 250 (f_{pu} = 1723 MPa) seven-wire prestressing strand (one column was tested using single-wire Grade 270 transverse reinforcement).

The testing consisted of three phases:

1. Three shear-critical columns (HS1 to HS3) were tested quasistatically at two axial load levels and incorporated either single-wire or seven-wire transverse reinforcement;
2. Four flexure-critical columns (HS5 to HS8) were tested at two different volumetric ratios of high-strength transverse reinforcement; one quasistatic and one dynamic test were performed at each reinforcement level; and
3. Two columns (HS9 and HS10), identically under-reinforced for shear to induce ductile shear failure, were tested to examine the effects of dynamic loading on mobilization of the transverse reinforcement in shear. HS9 was tested quasistatically, and HS10 dynamically.

The columns tested during first two phases were compared to conventionally reinforced columns. Comparison was made between HS1 and HS3, and NH3 (Vu et al.[14]), and HS2 with NH1.[14] The reference for flexural tests HS5 to HS8 was built at the time HS5 and HS6 were built, and was designated HS4. Table 1 summarizes reinforcement.

Day-of-test material properties and axial loads are shown in Table 2. Both concrete and steel strengths were taken as the average of three samples each.

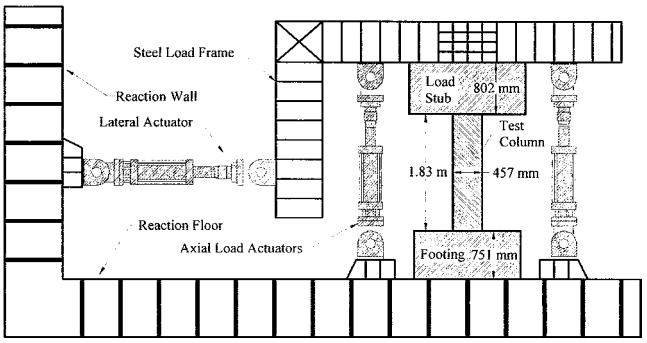

(a)

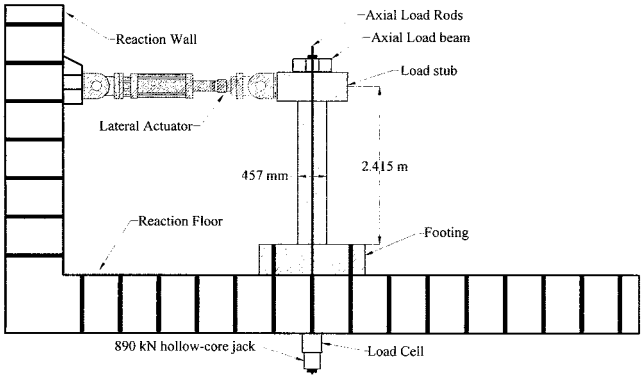

(b)

Fig. 2—(a) Installation for shear testing: HS1 to HS3, HS10, and NH1 and NH3; and (b) installation for flexural testing: HS4 to HS8.

QUASISTATIC AND DYNAMIC SHEAR TESTS

HS1-3 and HS9-10 were 457 mm diameter columns loaded in double bending (Fig. 2(a)), with a clear column height of 1.83 m (4*D*). HS1-3 was designed for shear according to the UCSD shear strength assessment model. This model was developed to realistically assess the shear capacity of existing columns; a 15% more conservative model is used for design. It was anticipated that the columns would fail in flexure.

In the UCSD model, theoretical shear strength of a circular section is given by[15]

$$V_d = V_c + V_s + V_p \quad (5)$$

in which V_c is the concrete shear-resisting mechanism, V_s is provided by the steel truss mechanism, and V_p is an enhancement from axial load forming, in a column in double bending, a diagonal compression strut on an angle α between the column axis and the centers of flexural compression in the end regions:

$$V_c = 0.29\alpha\beta\sqrt{f'_c}\,A_e \text{ for } \mu_\Delta \le 2 \text{ (MPa units)} \quad (6a)$$

$$V_c = 0.05\alpha\beta\sqrt{f'_c}\,A_e \text{ for } \mu_\Delta \ge 8 \text{ (MPa units)} \quad (6b)$$

$$V_s = \frac{\pi}{2}\frac{A_h f_{yt}(D-c-x)}{s}\cot\theta \quad (\theta = 30°) \quad (7)$$

$$V_p = P_e \tan\alpha_p \quad (8)$$

Table 1—Test unit reinforcement details

Test unit	Type	Longitudinal reinforcement (Grade 60)	ρ_l	Transverse reinforcement (Grade 250)	s, mm	ρ_t
HS1	Shear	20 No. 5 (D15.9)	0.025	6.2 mm strand	50	0.43%
HS2	Shear	20 No. 5 (D15.9)	0.025	6.2 mm strand	50	0.43%
HS3	Shear	20 No. 5 (D15.9)	0.025	4.4 mm strand (Grade 270)	35	0.43%
HS5,7	Flexure (HS7 dynamic)	20 No. 5 (D15.9)	0.025	6.2 mm strand	36.5	0.57%
HS6,8	Flexure (HS8 dynamic)	20 No. 5 (D15.9)	0.025	6.2 mm strand	69	0.32%
HS9,10	Shear (HS10 dynamic)	20 No. 6 (D19)	0.035	6.2 mm strand	100	0.22%
Reference tests						
NH1	Shear	20 No. 5 (D15.9)	0.025	No. 3 (D9.5) Grade 60	60	1.1%
NH3	Shear	20 No. 5 (D15.9)	0.025	No. 3 (D9.5) Grade 60	60	1.1%
NH4	Flexure	20 No. 5 (D15.9)	0.025	No. 3 (D9.5) Grade 60	86	0.8%

Table 2—Day-of-test material properties and axial load for HS1 to HS8, NH1, and NH3

Test unit	Column strength f'_c, MPa	Longitudinal steel strength, MPa		Transverse steel strength, MPa		Axial load, kN	Axial load ratio P_e/f'_cA_g
		Yield	Ultimate	Yield	Ultimate		
HS1	37.2	442.0	720.0	1569	1908	917	0.150
HS2	37.5	442.0	720.0	1569	1908	1847	0.300
HS3	39.1	442.0	720.0	1378	1757	962	0.150
HS5	32.5	429.2	720.0	1569	1908	794	0.149
HS6	34.3	429.2	720.0	1569	1908	815	0.144
HS7	34.2	429.2	720.0	1569	1908	836	0.149
HS8	35.9	429.2	720.0	1569	1908	848	0.144
HS9	46.8	446.9	735.6	1569	1908	935	0.121
HS10	47.1	446.9	735.6	1569	1908	934	0.121
Reference tests							
NH1	38.3	427.5	695	430.2	N/A	1885	0.300
NH3	39.4	427.5	695	430.2	N/A	969	0.150
HS4	32.0	429.2	720	385.8	812.3	793	0.151

where

$1 \le \alpha$ = $3 - M/VD \le 1.5$;
β = $0.5 + 20\rho_l \le 1$;
f'_c = concrete strength;
A_e = $0.8A_{gross}$;
A_h = area of transverse bar;
f_{yt} = yield strength of transverse bar;
D = column diameter;
c = clear cover to spiral;
x = neutral axis depth;
s = spiral pitch;
θ = angle of shear cracks to column axis;
α_p = angle between column axis and line connecting centers of compression zones (double bending); and
P_e = axial load.

The shear strength given by Eq. (6) to (8) is intended to provide a best estimate of strength and is to be used in assessment situations. A more conservative version is used for design.[5]

Table 3—Shear column test unit theoretical shear strength

Test unit	UCSD model $\mu_\Delta \leq 2$, kN	UCSD model $\mu_\Delta = 8$, kN	ATC-32, kN	ACI 318-99, kN	Maximum shear predicted, kN
HS1	776	583	432	585	548
HS2	858	664	487	656	603
HS3	787	589	437	595	546
HS9	594	410	289	441	586
HS10	595	411	290	442	587
NH1	939	743	524	674	570
NH3	802	604	469	607	516

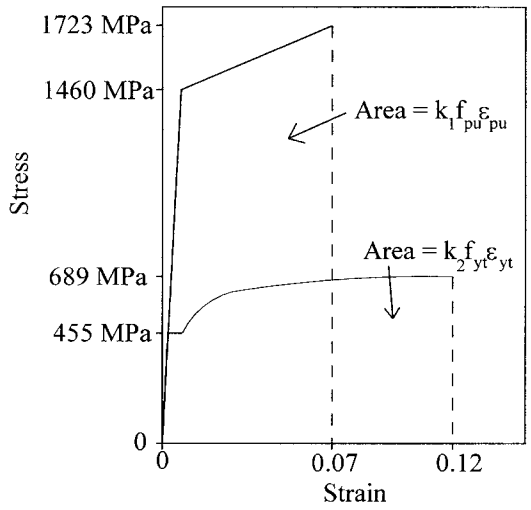

Fig. 3—Theoretical stress-strain curves for Grade 60 and 250 steel.

Transverse reinforcement was specified using nominal transverse steel strength of 1033 MPa ($0.6f_{pu}$). This value was chosen to keep the reinforcement well within the elastic range and limit crack widths. The volumetric transverse reinforcement ratio was 0.0043.

The shear design methodology outlined in ACI 318 utilizes a similar approach in considering contributions from concrete and steel mechanisms. The nominal shear strength

$$V_n = V_c + V_s \tag{9}$$

where

$$V_c = 2\left(1 + \frac{N_u}{13.8A_g}\right)\sqrt{f'_c}A_e \quad \text{(MPa units)} \tag{10}$$

in which N_u is the axial load, and the effective column area A_e is 0.8 times the column diameter times the section depth.

$$V_s = \frac{A_v f_{yt} d}{s} \tag{11}$$

where the total transverse bar area in a section and transverse bar yield strength are given by A_v and f_y, respectively, and d is the effective section depth (0.8 times the diameter).

Table 3 gives the predicted demand and theoretical shear strengths of HS1-3, 9, 10, NH1, and NH3, calculated using the UCSD model, ATC-32 (using Eq. (3) and (4)), and ACI 318 (the assumed yield for prestressing strand was $0.6f_{pu}$, to limit crack width).

A comparison can be made with design guidelines issued by the manufacturer for Ulbon,[16] and those suggested by Li et al.[7] Using the maximum volumetric reinforcement ratio of 0.006 and allowable tensile stress of 590 MPa specified by the manufacturer, Ulbon would not supply the required shear strength; for instance, a counterpart of HS1 reinforced with $\rho_t = 0.006$ Ulbon would have a nominal maximum shear strength at $\mu = 4$ of 462 kN. The maximum design stress suggested by Li et al. of 900 MPa would give a shear strength at $\mu = 4$ of 611 kN, which would be sufficient.

HS9 and HS10 were designed to fail in ductile shear at a displacement ductility level of 3.

STATIC AND DYNAMIC FLEXURAL TESTS

The test configuration for HS4 to HS8 in Fig. 2(b) provided an aspect ratio of 5.28 (column diameter 457 mm, length 2.415 m).

The volumetric ratio of transverse steel in reference test unit HS4 was determined using the equation developed by Priestley, Seible, and Calvi,[5] and adopted by ATC-32 to ensure adequate ductile performance:

$$\rho_t = 0.16\frac{f'_c}{f_{yt}}\left(0.5 + \frac{1.25P_e}{f'_c}\right) + 0.13(\rho_l - 0.01) \tag{12}$$

where

f'_c = unconfined concrete compressive strength;
f_{yt} = yield strength of transverse reinforcement;
P_e = applied axial load; and
ρ_l = longitudinal reinforcement ratio.

Use of the equation would have required a transverse reinforcement ratio of 0.009; however, a lower value of 0.008 was chosen to ensure that flexural failure would occur within the stroke capacity of the actuator. This resulted in the use of Grade 60 No. 3 spirals (413 MPa nominal yield) at 86 mm pitch ($s = 5.4d_{bl}$).

Design of transverse reinforcement in HS5 and HS7 used the equivalent strain energy approach developed by Mander et al.,[17] in which it was assumed that all of the strain energy absorbed by the transverse reinforcement to an ultimate strain of 0.07 would be available to balance the compressive strain energy of the concrete at maximum concrete compressive strain. The modified Mander expression for ultimate concrete compression strain is[5]

$$\varepsilon_{cu} = 0.004 + \frac{1.4f_{yt}\varepsilon_{ut}\rho_t}{f'_{cc}} \tag{13}$$

in which f'_{cc} is the compressive strength of confined concrete (taken in a simplified model as $1.5f'_c$). The transverse steel strain energy in this equation is proportional to the product $f_{yt}\varepsilon_{ut}$. For a given value of ε_{cu} obtained through the use of Grade 60 transverse reinforcement, one can replace $f_{yt}\varepsilon_{ut}$ with an equivalent strain energy term reflecting the properties of high-strength steel. Accordingly, the areas under the stress-strain curves of Grade 250 and Grade 60 reinforcement were set equal (Fig. 3) to achieve the following relationship:

$$f_{pu}\varepsilon_{pu} = \frac{k_2}{k_1} f_{yt}\varepsilon_{ut} \quad (14)$$

where

f_{pu} = ultimate strength of high-strength reinforcement (1723 MPa);

ε_{pu} = ultimate strain of high-strength reinforcement (0.07);

f_{yt} = expected yield strength of Grade 60 reinforcement (455 MPa);

ε_{ut} = ultimate strain of Grade 60 reinforcement (0.12); and

k_1, k_2 = constants (see Fig. 3; $k_1 = 0.87$, $k_2 = 1.34$).

Substituting from Eq. (14) into Eq. (13), the ultimate concrete compression strain is

$$\varepsilon_{cu} = 0.004 + \frac{0.877 f_{pu}\varepsilon_{pu}\rho_t}{f'_{cc}} \quad (15)$$

The manufacturer's quoted material properties for the prestressing strand were used. Concrete strength f'_c was taken as 34.5 MPa. The steel properties in the Mander model for confined concrete[17] were used,[18] assuming yield strain of 0.002276 at 455 MPa, a yield plateau to a strain of 0.008, and a parabolic strain hardening path to an ultimate strain of 0.12 at 689 MPa. Design transverse reinforcement ratio for HS5/7 was $\rho_t = 0.0057$.

The transverse reinforcement of HS6 and HS8 was designed to achieve ultimate confining pressure equivalent to that of HS4. Confining pressure provided by spiral reinforcement is

$$f_t = \frac{2 f_{ut} A_{sp}}{D's} \quad (16)$$

where

A_{sp} = area of transverse bar;

f_{ut} = spiral steel ultimate stress;

D' = spiral diameter to center of spiral; and

s = spiral pitch.

This relates to the volumetric transverse reinforcement ratio,

$$\rho_t = \frac{4A_{sp}}{D's} \quad (17)$$

to give

$$f_t = 0.5\rho_t f_{ut} \quad (18)$$

An increase in ultimate strength of the prestressing steel permits a significant reduction in the volumetric ratio of confinement. For the ultimate confining pressure in HS6 and HS8 to be equal to that of HS4, the required volumetric ratio of confinement in HS6 and HS8 would be

$$\rho_s = 0.008\frac{f_{ut}}{f_{pu}} = 0.008 \times \frac{689 \text{ MPa}}{1723 \text{ MPa}} = 0.0034 \quad (19)$$

SHEAR TEST PROCEDURE

The testing of HS1 to HS3 and HS9 was quasistatic and cyclic. The loading was carried out in load control up to first yield of the flexural reinforcement. A value for the displacement ductility $\mu = 1$ was calculated, extrapolating the line from the origin of the force-displacement response through the first-yield experimental response to the nominal strength. Displacement levels were chosen such that there would be a 50% increase per step to minimize low-cycle fatigue at low ductility levels. Three full cycles were performed at each level of ductility, to observe the stability of the hysteresis loop.

HS10 was tested dynamically. Cyclic loading through each displacement step of one or three cycles was performed as a separate dynamic event. A soft start (slow acceleration of the actuator to full speed, through an extra half-cycle of displacement) was used in the early (single) cycles; a hard start was used thereafter, in which the actuator was accelerated at its full capacity to maximum speed. Frequencies ranged from 2Hz at small displacements, to 0.6 Hz at a displacement ductility of 8.

FLEXURAL TEST PROCEDURE

The loading history for the flexural columns HS4, HS5, and HS6 followed the same general pattern described for the shear columns.

Dynamic testing of HS7 and HS8 followed the same displacement pattern as the quasistatic tests. The rate of cycling was at 2 Hz through $\mu = 1.5$, and as the stiffness decreased with the formation of a plastic hinge. The frequency was progressively reduced to a final value of 0.3 Hz at $\mu = 8$. Although the reduction in cycling frequency was, in part, imposed as a consequence of limitations on maximum loading velocity, it is realistic because the actual effective frequency of a ductile system reduces in proportion to $(\mu_\Delta)^{-0.5}$.[5] A hard start was used for HS7. For HS8, a soft start was chosen. The extra half-cycles that HS8 underwent using a soft start did result in its early failure.

SHEAR TEST RESULTS

The force-displacement hysteretic response of HS1 ($\rho_{axial} = 0.15 f'_c A_g$) is shown in Fig. 4. Energy absorption was excellent through $\mu = 10$, as evidently wide and stable hysteresis loops. Failure was initiated during the third cycle at $\mu = 10$, during which a spiral strand in the plastic hinge began to fray (individual wires broke within the seven-wire strand). Subsequently, the damaged spiral ruptured completely, allowing severe buckling of longitudinal bars.

A comparison with NH3 (Fig. 4) shows that the performance of NH3 was similar through $\mu = 8$. Confinement failure occurred during the third cycle at this ductility level.

The force-displacement response of HS2 (Fig. 5) displays stable response through $\mu = 8$. However, a spiral in the plastic hinge region began to fray at this level of ductility, allowing buckling of the longitudinal bars and a drop in the lateral capacity. The buckled bars ruptured en route to the first displacement peak at $\mu = 10$. HS2 is shown at $\mu = 8$ in Fig. 6.

The reference column for HS2, NH1 (Fig. 5), showed stable ductile response through $\mu = 6$. Direct comparison at higher levels of ductility is not possible because of an equipment failure in NH1.

HS3, which differed from HS1 in the use of single-wire Grade 270 transverse reinforcement, showed performance similar to HS1 through $\mu = 6$ (Fig. 7). A spiral in the upper plastic hinge region fractured at the first negative displace-

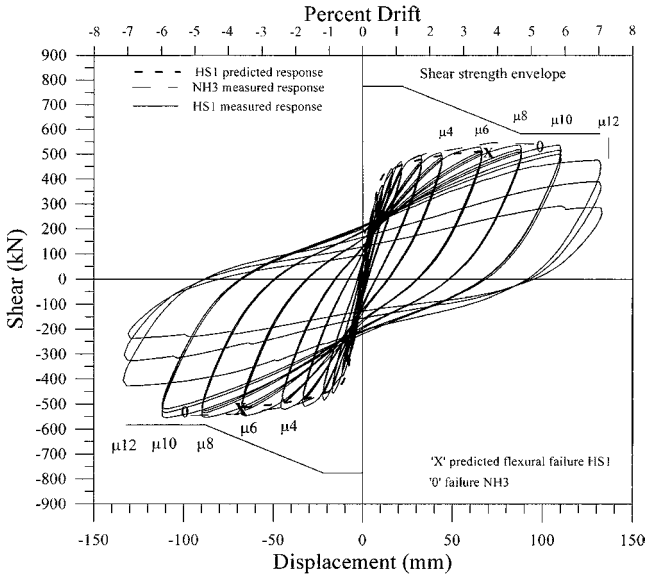

Fig. 4—Force-displacement response of HS1 (seven-wire Grade 250; $P_e/f_c'A_g = 0.15$).

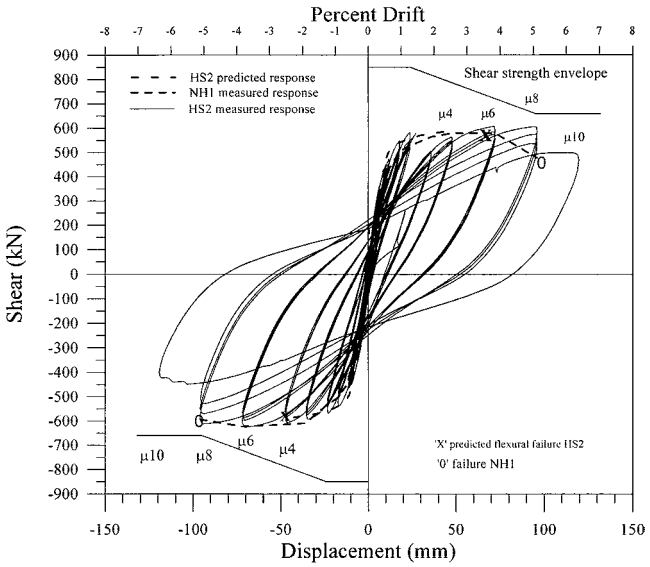

Fig. 5—Force-displacement response of HS2 (seven-wire Grade 250; $P_e/f_c'A_g = 0.30$).

ment peak of μ = 8, which allowed longitudinal bar buckling and subsequent failure.

Visual examination of the columns during the course of the tests showed some differences from conventionally reinforced members at high ductility levels. Longitudinal bar buckling was not as pronounced at equivalent levels of displacement ductility because the spirals had a longer elastic range. The fractured ends of the failed spiral rebounded (pulled far apart) after failure.

In all three columns, shear cracking was extensive; however, outside the plastic hinge region, shear cracks were elastic, and closed upon removal of lateral force.

Measured strains in transverse steel at peak ductility levels are shown for HS1 HS2, and HS3 in Fig. 8, 9, and 10, respectively. Yield on the figures is considered as the strain at $0.85f_{pu}$, generally considered the beginning of the inelastic regime. The profiles show peak strain occurring at approximately $0.75D$

Fig. 6—HS2 at m = 8.

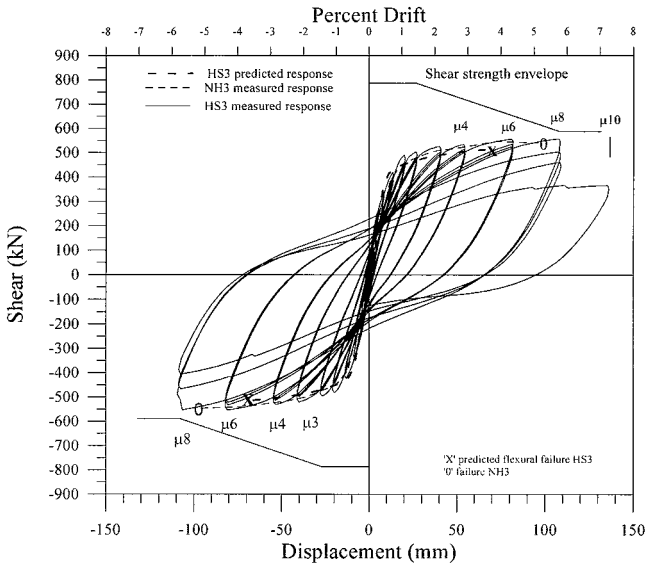

Fig. 7—Force-displacement response of HS3 (single-wire Grade 270; $P_e/f_c'A_g = 0.15$).

from the top and bottom of the column. In the central region, away from the plastic hinge region, transverse reinforcement strains were much lower as a result of reduced crack widths. At the base and the top of the column, confinement provided by the foundation and load stub respectively restricts radial dilation, and hence, shear strains are also reduced in these regions. It is noticeable that the region of high shear strain extends further from the plastic hinge section with the column HS3, which was transversely reinforced with smooth wire, than with HS1 and HS2, which were confined with strand. The reason for this is not clear, but it may be due to strain penetration from high confinement strains in the

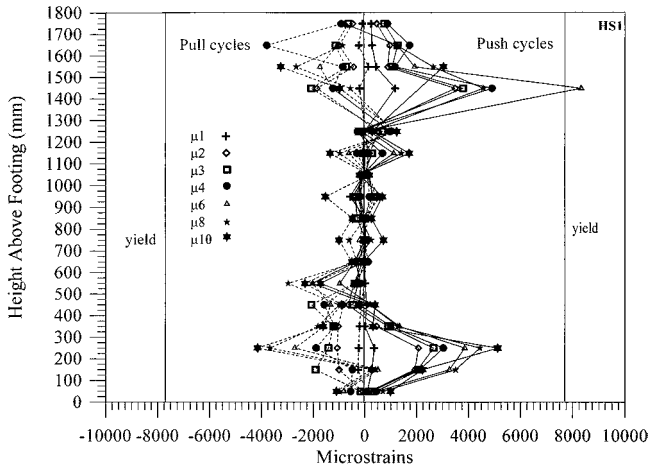

Fig. 8—Transverse steel strains on shear face of HS1 (seven-wire Grade 250; $P_e/f_c'A_g = 0.15$).

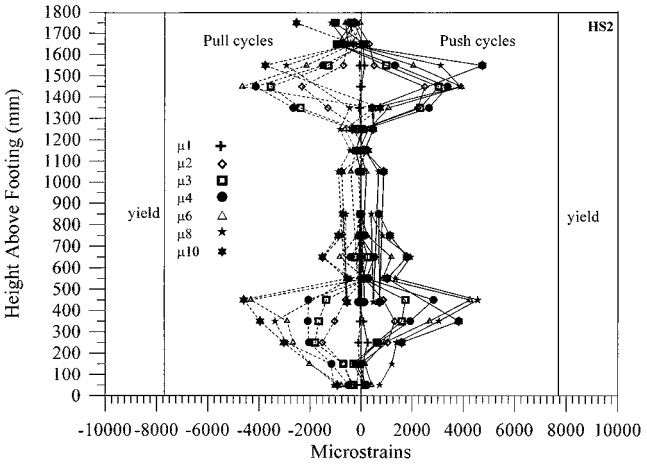

Fig. 9—Transverse steel strains on shear face of HS2 (seven-wire Grade 250; $P_e/f_c'A_g = 0.30$).

hinges on the loading faces. The strains developed there may extend to the column sides as a consequence of the poor bond characteristics of the smooth wire.

The recorded peak strains correspond to peak stresses of 900 to 1100 MPa, except at ductility $\mu_\Delta = 10$ when confinement failure occurred (causing higher strains). This agrees well with the design value of 1033 MPa.

The force-displacement response of HS9 and 10 is shown in Fig. 11. It may be seen that the peak shear carried by HS10 (at $\mu = 3$) coincided both with the predicted response and the UCSD shear envelope prediction. The loss of strength beyond this point was rapid. Significant shear cracking was observed shortly after $\mu = 1$. The response of HS9, as shown by the envelope, was similar, with a slightly lower peak shear (HS10's was higher due to dynamic effects).

The shear actual versus predicted shear strength of each test, shown in Table 3, shows some interesting results. While both the UCSD degrading shear strength model and ACI 318 successfully predicted the satisfactory performance of HS1 to HS3, the equation from ATC-32 did not, underpredicting shear strength by approximately 20%. The performance of HS9 and HS10 was likewise well-predicted by the UCSD model, while in this case, both ACI 318 and ATC-32 underpredicted it (Table 3 and Fig. 11). It is clear that a degrading

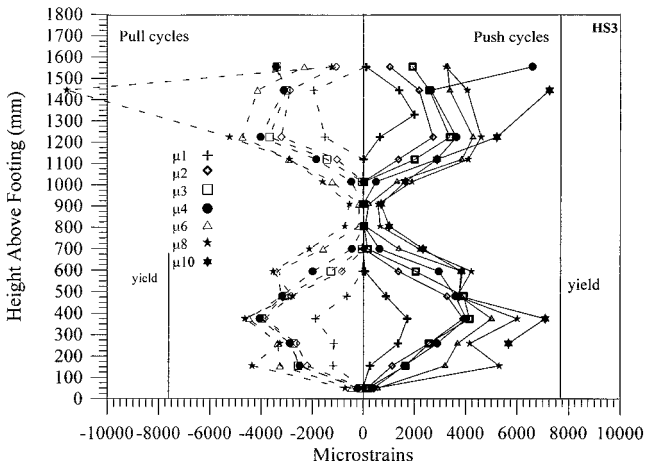

Fig. 10—Transverse steel strains on shear face of HS3 (single-wire Grade 270; $P_e/f_c'A_g = 0.15$).

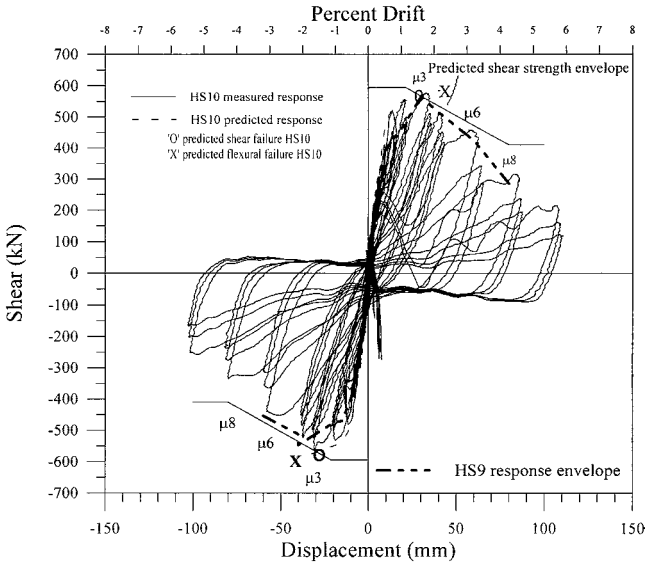

Fig. 11—Force-displacement response of HS9 and HS10 (designed for shear failure: HS9, quasistatic; HS10, dynamic).

shear-strength model correctly predicts the response of columns reinforced with this material.

FLEXURAL TEST RESULTS

The force-displacement response of HS5 is shown in Fig. 12. Also in Fig. 12 is the response envelope of the reference test, HS4. HS5 showed wide and stable hysteresis loops through three cycles at $\mu = 8$, with no visible damage to the reinforcing steel. On the first displacement peak at $\mu = 10$, three longitudinal bars experienced mild buckling over several spiral turns. Fraying of one spiral and more longitudinal bar buckling occurred during the first negative peak at $\mu = 10$. HS5's performance remained stable through the second displacement peak at this level of ductility, but reversal of load from this point saw rapid failure through strand and longitudinal bar rupture. During cycling at $\mu = 6$ and $\mu = 8$, the footing cover concrete was undergoing considerable spalling, indicating that the effectiveness of the confinement about the column hinge was forcing a significant degree of plasticity into the footing. HS5 is shown at $\mu = 10$ in Fig. 13, at the end of the first pull excursion. Damage to the footing is visible.

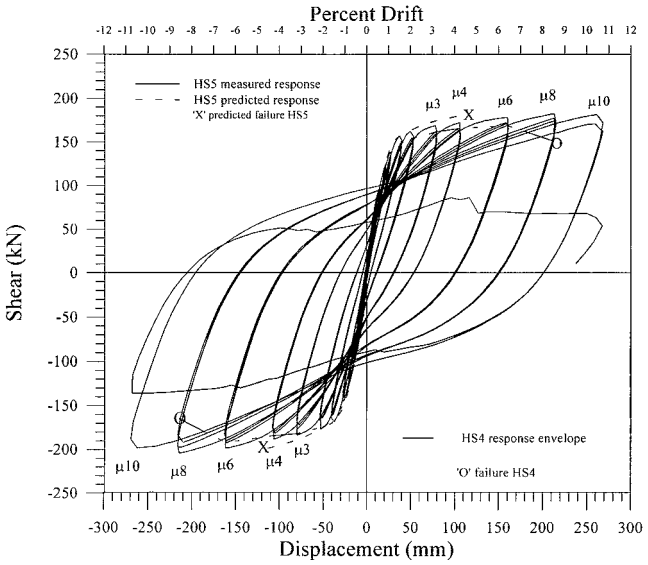

Fig. 12—Force-displacement response of HS5 (equivalent strain energy of transverse reinforcement.

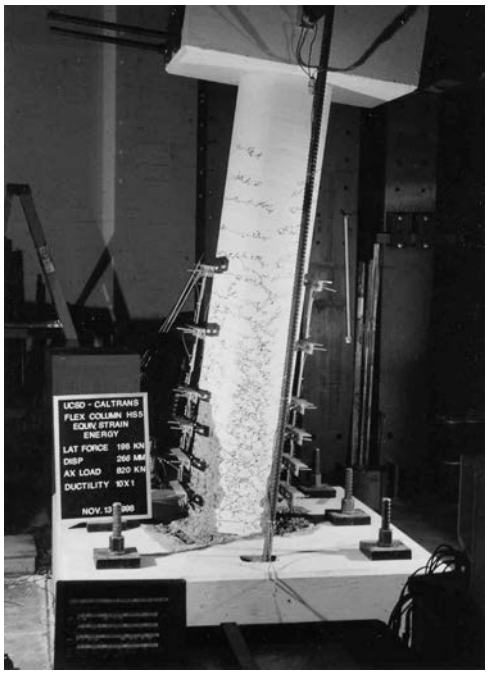

Fig. 13—HS5 at μ = 10.

HS4, in comparison, experienced longitudinal bar buckling at μ = 6, and failed during cycling at μ = 8. Light footing damage was seen in HS4.

Figure 14 shows the force-displacement response of HS6. The longitudinal steel in HS6 began to buckle during the last cycle at μ = 4. Buckling occurred between spirals; through μ = 6, no damage to the spirals was seen. Approaching the first displacement peak at μ = 8, two adjacent spirals began to fray, allowing severe and widespread buckling of the longitudinal steel, instigating failure.

Damage to HS6 occurred earlier than in HS4 and spread more rapidly, even though the transverse reinforcement had a smaller pitch (66 versus 86 mm). This may have been a result of the lower elastic modulus (189 versus 200 GPa for Grade 60) and smaller area of the prestressing strand (compared to solid bar), giving a reduced elastic stiffness against longitudinal bar buckling.

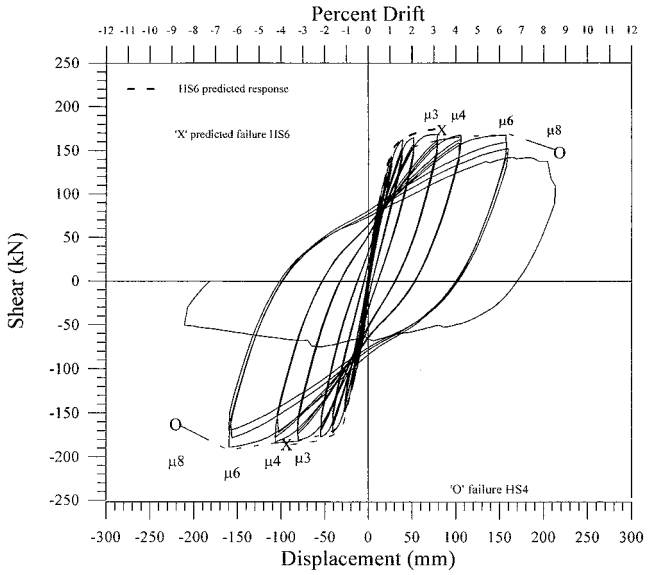

Fig. 14—Force-displacement response of HS6 (equivalent confining pressure).

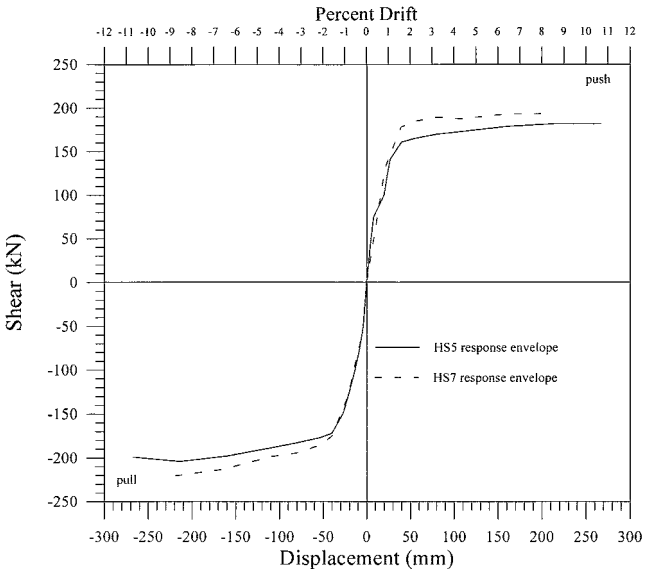

Fig. 15—Force-displacement response envelopes of HS5 (quasistatic) and HS7 (dynamic).

The force-displacement response envelopes of HS5 and HS7 are compared in Fig. 15. The strength of HS7 is approximately 8% greater than that of HS5 due to slightly greater concrete strength and dynamic amplification of the confined concrete strength.[17] The maximum strain rate at maximum strength was approximately 0.0133/s. At the end of three dynamic cycles at μ = 8, no damage to reinforcement was observed.

Force-displacement response envelopes for HS6 and HS8 are shown in Fig. 16. Use of the soft start to the loading of HS8 resulted in the column absorbing a greater amount of strain energy when compared to the other specimens. This resulted in failure at a lower level of ductility than HS6. The strain-rate enhancement of strength was minimal in HS8.

Strain gage data from the confinement in HS5 to HS8 indicate extensive mobilization. Strains remained in the elastic

range in HS5 and HS7, but inelastic strains were observed in HS6 and HS8.

CONCLUSIONS

Shear tests

Five model bridge columns with an aspect ratio of 2 were tested, at two levels of axial load, and using either stranded seven-wire or single-wire high-strength transverse reinforcement. The test units that were designed for adequate shear strength (HS1, HS2, and HS3) matched or exceeded the ductile performance recorded by conventionally reinforced columns. HS9 and HS10 were tested to investigate the effect of dynamic loading on shear failure in a column reinforced with seven-wire prestressing strand. They demonstrated that dynamic loading had little effect, and that ductile failure was softened by the fraying rupture of the strand.

The conclusions reached in the testing of HS1 to HS3, and HS9 and HS10 are as follows:

1. The observed response of the tested columns indicate that using a conservative value of $0.6f_{pu}$ for maximum allowable tensile stress in the transverse reinforcement provided adequate strength for the steel truss shear-resisting mechanism while significantly reducing steel congestion. Crack widths resulting from elastic deformation of the transverse reinforcement were not large enough to significantly degrade the concrete shear-resisting response;

2. The transverse reinforcement outside the plastic hinge regions remained in the elastic range, allowing the shear cracks outside the plastic hinge regions to close completely upon removal of load;

3. The transverse reinforcement in the plastic hinge regions remained, in general, within the elastic range; the strains recorded would have caused yielding in conventional reinforcement. The sustained elastic stiffness in confinement steel delayed the onset of longitudinal bar buckling and thereby contributed to HS1 and HS2 surpassing the performance of their conventionally reinforced counterparts;

4. The use of single-wire reinforcement in HS3 gave performance comparable to the level of Grade 60 reinforcement specified by the UCSD shear model;

5. The progressive, fraying rupture of the transverse strand softened the brittle shear failure in HS9 and HS10. The partially ruptured spirals could still carry load until high structural displacements were reached, and wide shear cracks opened. Both HS9 and HS10 eventually failed through degradation of the concrete component of the shear-resisting mechanism;

6. While only one dynamic shear test was performed, it was observed that shear failure induced by dynamic testing showed a slight delay in the onset of damage to the transverse reinforcement, but overall performance under dynamic loading was similar. This is an area that should be addressed through further work; and

A degrading shear strength model can successfully predict the behavior of columns reinforced with high-strength transverse reinforcement.

Flexural tests

Conclusions reached in the testing of model bridge columns HS5-HS8 are as follows:

1. The ability of high-strength strand to remain elastic in resisting core dilation resulted in good performance provided spiral pitch was sufficiently close to prevent buckling of the longitudinal reinforcement;

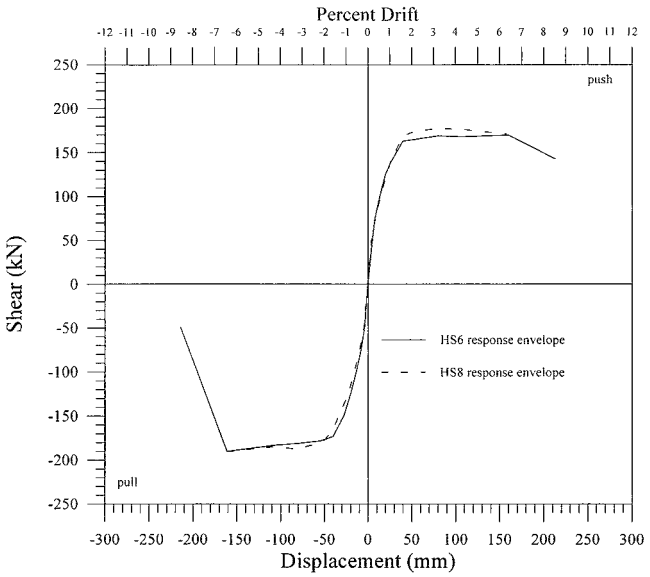

Fig. 16—Force-displacement response envelopes of HS6 (quasistatic) and HS8 (dynamic).

2. Designing transverse reinforcement using prestressing strand provides a greater rotational capacity in the plastic hinge than does conventional reinforcement if transverse steel strain energy capacity equivalent to that provided by Grade 60 is assumed for design;

3. Designing transverse reinforcement using prestressing strand for an inelastic confining pressure equivalent to that provided by Grade 60 will provide performance similar to that of conventional reinforcement at greatly reduced volumetric ratios, provided that antibuckling criteria are met;

4. Using prestressing strand as transverse reinforcement, a nominal spiral pitch of $s \leq 6d_{bl}$ was inadequate to forestall buckling of the longitudinal reinforcement. This was caused by: 1) the lower elastic modulus, and hence lower stiffness of prestressing steel; and 2) the reduced steel area of the seven-wire strand when compared to a solid bar. From the response of HS1 and HS2, which ultimately displayed a flexural response, it is suggested that $s = 4d_{bl}$ may be used in design. This is an area in which a need for further work is indicated; and

5. Though only two dynamic tests were performed, the results were consistent with those recorded by Mander et al. [15] Dynamic enhancement of the strength of concrete confined with high-strength transverse reinforcement was increased on the order of 8%.

ACKNOWLEDGMENTS

Special thanks to Florida Wire and Cable for donating the prestressing strand used in this project. The California Department of Transportation funded this project. The conclusions stated herein are solely those of the authors, and do not imply official sanction of the California Department of Transportation.

NOTATION

A_e = effective column cross-sectional area
A_g = column gross cross-sectional area
A_h, A_v = transverse steel area in given section (UCSD/ATC-32 and ACI 318, respectively)
A_{sp} = transverse spiral bar area
c = depth of concrete cover
D = column outside diameter
D' = diameter across transverse reinforcement
d = effective column diameter (ACI 318 shear model)
d_{bl} = diameter of longitudinal steel bars
f_l = confining pressure from transverse reinforcement

f_{pu} = ultimate strain of prestressing strand
f_{ut} = ultimate strength of prestressing strand
f_{ye} = expected yield strength of longitudinal reinforcement
f_{yl} = nominal yield strength of longitudinal reinforcement
f_{yt} = yield strain of transverse reinforcement
f_c' = compressive strength of unconfined concrete
f_{cc}' = compressive strength of confined concrete
f_{ce}' = expected compressive strength of unconfined concrete for seismic assessment
h_c = clear column height
k_1, k_1 = constants
M_n = nominal flexural strength
N_u = axial load (notation used in ACI 318 shear equation)
P_e = axial load (notation used in ATC-32 and UCSD shear equations)
s = spiral pitch
V^0 = shear demand (ATC-32)
V_c = concrete contribution of shear strength
V_d = shear strength of a section (UCSD model)
V_n = shear strength of section (ACI 318)
V_p = axial load enhancement of shear strength
V_s = steel contribution to shear strength
α = factor relating to shear span to concrete shear strength component
α_p = angel between column vertical axis and center of compression zone
β = factor relating to longitudinal reinforcement ratio to concrete shear strength component
ε_{cu} = maximum stress of confined concrete
ε_{pu} = ultimate strain of prestressing steel
ε_{ut} = ultimate stress of conventional reinforcing steel
Φ = overstrength factor
μ_Δ = displacement ductility
Θ = angle of shear cracks to column axis
ρ_l = volumetric ratio of longitudinal reinforcement
ρ_t = volumetric ratio of transverse reinforcement

REFERENCES

1. ATC-32, "Improved Seismic Design Criteria for California Bridges: Provisional Recommendations," Applied Technology Council, Redwood City, Calif., 1996.

2. Caltrans, "Bridge Design Specifications," California Department of Transportation, Sacramento, Calif., 1995.

3. Priestley, M. J. N., "Comments on ATC-32 Concrete Provisions," *Proceedings of the Fourth Annual Caltrans Seismic Workshop*, Sacramento, Calif., June 1996.

4. ACI Committee 318, "Building Code Requirements for Structural Concrete (ACI 318-99) and Commentary (318R-99)," American Concrete Institute, Farmington Hills, Mich., 1999, 391 pp.

5. Priestley, M. J. N.; Seible, F.; and Calvi, M., *Seismic Design and Retrofit of Bridges*, John Wiley & Sons, New York, 1996.

6. Pessiki, S.; Graybeal, B.; and Mudlock, M., "Proposed Design of High-Strength Spiral Reinforcement in Compression Members," *ACI Structural Journal*, V. 98, No. 6, Nov.-Dec. 2001, pp. 799-810.

7. Li, B.; Park, R.; and Tanaka, H., "Strength and Ductility of Reinforced Concrete Members and Frames Constructed Using High-Strength Concrete," *Research Report* No. 94-5, Department of Civil Engineering, University of Canterbury, Christchurch, New Zealand, May 1994.

8. Razvi, S. R., and Saatcioglu, M., "Circular High-Strength Concrete Columns under Concentric Compression," *ACI Structural Journal*, V. 96, No. 5, Sept.-Oct. 1999, pp. 817-825.

9. Muguruma, H.; Nishiyama, M.; Watanabe, F.; and Tanaka, H., "Ductile Behavior of High-Strength Concrete Columns Confined by High-Strength Transverse Reinforcement," *Evaluation and Rehabilitation of Concrete Structures and Innovations in Design*, SP-128, V. M. Malhotra, ed., American Concrete Institute, Farmington Hills, Mich., 1991, pp. 877-891.

10. Sato, Y.; Tanaka, H.; and Park, R., "Reinforced Concrete Columns with Mixed-Grade Longitudinal Reinforcement," *Research Report* No. 93-7, Department of Civil Engineering, University of Canterbury, Christchurch, New Zealand, Aug. 1993.

11. NZS 3101—*The Design of Concrete Structures—Part 1: Practice* and *The Design of Concrete Structures—Part 2: Commentary*, Standards Association of New Zealand, Wellington, New Zealand, 1982.

12. Aziznamini, A., and Saatcioglu, M., "Performance of High-Strength Concrete (HSC) Columns Confined with Rectilinear Reinforcement," *High-Strength Concrete in Seismic Regions*, SP-176, C. W. French and M. E. Kreger, eds., American Concrete Institute, Farmington Hills, Mich., 1998, pp. 213-235.

13. Watanabe, F., and Kabeyasawa, T., "Shear Strength of RC Members with High-Strength Concrete," *High-Strength Concrete in Seismic Regions*, SP-176, C. W. French and M. E. Kreger, eds., American Concrete Institute, Farmington Hills, Mich., 1998, pp. 379-396.

14. Vu, N.; Priestley, M. J. N.; Seible, F.; and Benzoni, G., "The Seismic Response of Well-Confined Circular Reinforced Concrete Columns with Low Aspect Ratios," *Report* No. SSRP-97/15, Department of Structural Engineering, University of California at San Diego, Feb. 1999.

15. Kowalsky, M. J., and Priestley, M. J. N., "Improved Analytical Model for Shear Strength of Circular Reinforced Concrete Columns in Seismic Regions," *ACI Structural Journal*, V. 97, No. 8, May-June 2000, pp. 388-396.

16. "Design Standard for Using High Tensile Steel ULBON as Shear Reinforcement in Reinforced Concrete Beams and Columns," Neturen Co., Ltd., Tokyo, Japan, 1988.

17. Mander, J.; Priestley, M. J. N.; and Park, R., "Observed Stress-Strain Behavior of Confined Concrete," *Journal of the Structural Division*, ASCE, V. 114, No. 8, Aug. 1988, pp. 1827-1849.

18. Scott, B. D.; Park, R.; and Priestley, M. J. N., "Stress-Strain Behavior of Concrete Confined by Overlapping Hoops at Low and High Strain Rates," ACI JOURNAL, *Proceedings* V. 79, No. 1, Jan.-Feb. 1982, pp. 13-27.